The Probability of Quantal Secretion Within an Array of Calcium Channels of an Active Zone

M. R. Bennett,* L. Farnell,† and W. G. Gibson†

*The Neurobiology Laboratory, Institute for Biomedical Research, Department of Physiology, and †The School of Mathematics and Statistics, University of Sydney, New South Wales 2006, Australia

ABSTRACT A Monte Carlo analysis has been made of calcium dynamics in submembranous domains of active zones in which the calcium contributed by the opening of many channels is pooled. The kinetics of calcium ions in these domains has been determined using simulations for channels arranged in different geometries, according to the active zone under consideration: rectangular grids for varicosities and boutons and lines for motor-nerve terminals. The effects of endogenous fixed and mobile buffers on the two-dimensional distribution of free calcium ions at these active zones are then given, together with the extent to which these are perturbed and can be detected with different affinity calcium indicators when the calcium channels open stochastically under an action potential. A Monte Carlo analysis of how the dynamics of calcium ions in the submembranous domains determines the probability of exocytosis from docked vesicles is also presented. The spatial distribution of exocytosis from rectangular arrays of secretory units is such that exocytosis is largely excluded from the edges of the array, due to the effects of endogenous buffers. There is a steeper than linear increase in quantal release with an increase in the number of secretory units in the array, indicating that there is not just a local interaction between secretory units. Conditioning action potentials promote an increase in quantal release by a subsequent action potential primarily by depleting the fixed and mobile buffers in the center of the array. In the case of two parallel lines of secretory units exocytosis is random, and diffusion, together with the endogenous calcium buffers, ensures that the secretory units only interact over relatively short distances. As a consequence of this and in contrast to the case of the rectangular array, there is a linear relationship between the extent of quantal secretion from these zones and their length, for lengths greater than a critical value. This Monte Carlo analysis successfully predicts the relationship between the size and geometry of active zones and the probability of quantal secretion at these, the existence of quantal versus multiquantal release at different active zones, and the origins of the F1 phase of facilitation in synapses possessing different active zone geometries.

INTRODUCTION

There is considerable evidence to suggest that secretory units may be the units of quantal secretion at some terminals but not at others (see the accompanying paper, Bennett et al., 2000). For example, quantal secretion from the calyx terminal of the rat medial nucleus is attenuated by introduction of the relatively slow buffer ethylene glucol-bis(β-aminoethyl ether)-*N*,*N*,*N*′,*N*′-tetraacetic acid (EGTA), which is only slightly less efficient than 1,2-bis(2-aminophenoxy)ethane-*N*,*N*,*N*,*N*-tetraacetic acid acetoxymethyl ester (BAPTA) in reducing secretion (Borst and Sakmann, 1996). This observation suggests that it is the slower accumulation of calcium from many channels in the vicinity of the calcium sensor, rather than just a strategically placed channel within the secretory unit, that is responsible for triggering secretion. The contribution of calcium from many channels at the presynaptic membrane forms a "submembranous calcium domain" that extends over the region of calcium entry into the terminal (Klingauf and Neher, 1997). In contrast to the microdomain, in which the calcium dynamics is dominated by diffusion rather than buffering, the opposite is the case in the submembranous domain. Furthermore, the calcium concentration in this domain is, in addition to the endogenous buffers, determined by the spatial layout of the calcium channels in the domain, that is, in the arrangement of channels in the active zone of the nerve terminal. The two most distinct geometries of active zones are those found on the one hand in the amphibian motor nerve terminal, in which the docked vesicles and channels occur on a line (Heuser and Reese, 1973; Robitaille et al., 1990), and on the other hand in boutons in which they appear to be arranged in a regular two-dimensional array (Pfenninger et al., 1972). A Monte Carlo analysis has therefore been carried out on the dynamics of calcium movement in submembranous domains associated with active zones possessing either of these two geometries, in the presence of both mobile and fixed endogenous buffers and either low- or high-affinity indicators, when calcium channels open under an action potential. Consideration is also given as to how this calcium interacts stochastically with the different spatial distributions of docked vesicles that are found in the active zones of varicosities, boutons, and motor-nerve terminals. This further Monte Carlo analysis then provides estimates of the probabilities of quantal release at these synapses.

Received for publication 6 November 1998 and in final form 20 January 2000.

Address reprint requests to Dr. M. R. Bennett, Neurobiology Laboratory, F13, University of Sydney, NSW 2006, Australia. Tel.: 61-2-9351-2034; Fax: 61-2-9351-3910; E-mail: maxb@physiol.usyd.edu.au

0006-3495/00/05/2222/19 $2.00

METHODS

The application of the Monte Carlo simulation method to the influx, diffusion, and binding of calcium in a terminal for the case where only one

calcium channel opens has been given in detail in the accompanying paper (Bennett et al., 2000, hereafter referred to as I.) The extension required here is to the case where multiple calcium channels can open under an action potential.

The way in which a single channel opens under a Hodgkin-Huxley action potential was investigated in detail in Bennett et al. (1997). There, the opening and closing times, t_{open} and t_{close}, were modeled as nonhomogeneous Poisson processes with rate parameters that depended on the action potential, and hence were functions of time. The single-channel calcium current, $i_c(t)$, was also expressed as a function of the potential. All parameter values were based on the N-channel data of Delcour et al. (1993). The problem is how to incorporate multiple channels into the Monte Carlo scheme. To include the full details would make the simulation extremely complicated and time-consuming: each channel would open and close stochastically and the currents through the open channels would have to be continuously varied during the course of the action potential. However, to assume all channels open synchronously and admit constant current would be a serious distortion of the true situation. A compromise is to divide the time of the action potential into subintervals of length δt, to estimate the proportion of channels that are open in each subinterval, and to assume the single-channel current has a constant value through a subinterval. The proportion of channels open in a given subinterval can be estimated from simulations using the continuous theory as given in Bennett et al. (1997). In addition, the total charge δq through a typical channel in a given subinterval $[n\delta t, (n + 1)\delta t]$ can be found from simulations using the formula

$$\delta q = \int_{n\delta t}^{(n+1)\delta t} i_c(t)g(t)dt, \qquad (1)$$

where $i_c(t)$ is the single channel current and $g(t)$ is 1 if the channel is open and 0 otherwise; from this one calculates the average current per channel in the subinterval $[n\delta t, (n + 1)\delta t]$ as $\delta q/\delta t$. The results of this calculation, using $\delta t = 0.5$ ms, are given in Table 1; the parameters used in the simulations are the same as in Bennett et al. (1997), except that the single-channel calcium current $i_c(t)$ has been reduced to half the value given there (see the discussion of parameter values in Paper I). Also shown in Table 1 are the actual number of open channels assumed if a total array of 64 channels is used. Another approximation made in the use of this scheme is that the channels open in any subinterval are chosen at random from the total array of channels; that is, no attempt is made to track the opening behavior of individual channels across subintervals. The effect of this is to give fewer long openings than actually occur under an action potential. To estimate the error caused by this approximation, a number of runs were also done where it was assumed that if a channel is open in a given interval δt, it has double the normal probability of being open in the next interval (with, however, still the same total number of channels open in a given interval). This caused only a small increase in the number of exocytotic events occurring, and it is concluded that this approximation is in keeping with the general level of approximation made elsewhere.

TABLE 1 A discrete approximation for calcium entry through the plasmalemma under an action potential

Interval (ms)	Mean fraction of open channels	Number of open channels of 64	Average current per open channel (pA)
(0, 0.5)	0.0064	0	0.12
(0.5, 1.0)	0.0342	2	0.05
(1.0, 1.5)	0.3010	19	0.03
(1.5, 2.0)	0.3535	23	0.08
(2.0, 2.5)	0.2758	18	0.14
(2.5, 3.0)	0.1562	10	0.17
(3.0, 3.5)	0.0555	4	0.19
(3.5, 4.0)	0.0080	1	0.15
(4.0, 4.5)	0.0019	0	0.07

The action potential commences at time 0, and the duration time is divided into 0.5-ms subintervals. The second column gives the mean fraction of calcium channels that are open in each subinterval and the third column translates this into an actual number for the particular case where there are a total of 64 calcium channels present. The last column gives the average current passing through each open channel in that subinterval, calculated using half the single channel current given in Delcour et al. (1993); this will be referred to as the "standard calcium current" case. Some calculations are also done using twice this current, which means that they are based on the single channel current of Delcour et al. (1993).

The parameter values for the kinetics of quantal secretion are the same as those given in Table 1 of Paper I (Bennett et al., 2000). The attachment rate for calcium binding to the sensor protein (k^a; 15×10^6 M^{-1} s^{-1}) and the conformational change in the protein (β; 2000 s^{-1}) are similar to those for the kinetics of secretion at retinal bipolar cell synapses (14×10^6 M^{-1} s^{-1} and 2000 s^{-1}; Heidelberger et al., 1994) as well as for secretion from neuroendocrine cells (14×10^6 M^{-1} s^{-1} and 1000 s^{-1}; Heinemann et al., 1994). The detachment rate (k^d; 750 s^{-1}) used in this study is drawn from a range of synapses and cell types (see Table 2 in Bennett et al., 1997). The application of our kinetic model with these parameters to experimental data from neuromuscular synapses is contingent on the quantal release process at these synapses possessing similar kinetics and parameter values as those appropriate for bipolar synapses and neuroendocrine cells.

RESULTS

The Monte Carlo results are divided into two main sections. The first of these investigates the calcium transients at the presynaptic membrane when there are multiple calcium channel openings, as occurs under an action potential. The second section is concerned with using the information provided by the previous section to establish how calcium transients from different arrays of channels affect the triggering of vesicle exocytosis following an action potential, when these vesicles are arranged in different configurations with respect to the channels. In all cases the terminal contains a mobile buffer with the characteristics of calmodulin and a fixed buffer with the characteristics of calbindin (see Table 1 in Paper I). In addition, a calcium indicator is sometimes present, which is either furaptra, representative of a low-affinity indicator, or fura-2, representative of a high-affinity indicator. Unless otherwise mentioned, all values of free calcium and of calcium bound to the various buffers are the means of at least five simulation trials. It is made explicit when the standard deviations of these are given.

Ca^{2+} transients under an action potential

In varicosities and boutons

A submembranous calcium domain refers to a volume at the active zone of a terminal within which the pooled calcium, arising from the opening of a number of channels in the zone under an action potential, may be sufficient to trigger the exocytosis of vesicles whether or not they possess a

nearby channel that is opened by the action potential. Monte Carlo calculations have therefore been made to determine the spatial distribution of the mean and variance of the peak free calcium concentration at the presynaptic membrane of a varicosity or bouton in such a submembranous domain. A volume of cytosol in a terminal was considered that was made up of a 1 μm $\times$ 1 μm square base of presynaptic membrane and taken to a height of 30 nm from the membrane (Fig. 1). In the absence of quantitative information concerning the spatial arrangement of calcium channels in boutons (see Westerbroek et al., 1995), channels that occupied the active zone region were arranged in the middle of this presynaptic membrane. Given that there is some knowledge concerning the spatial distribution of vesicles in the active zones of boutons, and that according to the secretory unit hypothesis these vesicles are associated with calcium channels, the active zone has been modeled as a square array of vesicles and their associated channels placed on a regular grid (Fig. 1; see also Fig. 7 *A*). The separation between the channels has been set at 70.7 nm (giving a diagonal separation of 100 nm) and two array sizes have been used, containing 5 $\times$ 5 and 9 $\times$ 9 channels, respectively.

The boundaries of the presynaptic membrane, that is, the other five sides of the varicosity or bouton, were closed by walls of membrane incorporating pumps, as described under Methods in Paper I. Previous calculations have shown that 0.46 of the N-type channels open on average under an action potential (Bennett et al., 1997), so this has been taken as the frequency in the present case. The spatial distribution of open channels occurs at random in each time interval of 0.5 ms during the action potential, and this has been arranged in such a way as to give a frequency distribution of open times that is similar to that expected for channels under an action potential (for details, see Methods above).

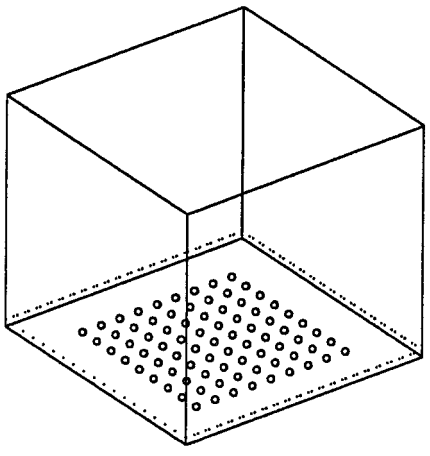

FIGURE 1 The Monte Carlo simulation typically uses a cubic box with 1000-nm sides. The plasmalemma is represented by the 1 μm $\times$ 1 μm base; vesicles and their associated calcium channels are placed in a regular array in the central region of this area (the figure shows a 9 $\times$ 9 array). Calcium pumps are situated on all six walls of the box. The submembranous domain is taken to extend to a height of 30 nm above the plasmalemma, as shown by the dotted line.

Fig. 2 shows the mean of the spatial distribution of the calcium ions at the time of peak calcium concentration in the volume under consideration. This is the average of the results for five action potentials. Two cases have been considered, one in which an active zone possesses a small array of channels (5 $\times$ 5; Fig. 2, *A* and *C*) and the other a large array (9 $\times$ 9; Fig. 2, *B* and *D*). At this time, the average number of calcium ions at any particular site (taken to be a cube of side 30 nm with one face in the presynaptic membrane) is generally much less than one, except at the middle of the zone (Fig. 2, *Aa* and *Ba*). This is mainly because of the removal of the calcium ions by the fixed buffer (Fig. 2, *Ac* and *Bc*), and to a lesser extent by the mobile buffer (Fig. 2, *Ab* and *Bb*). Even though the average number of calcium ions per site in the middle of the array is still only about one, this amounts to a calcium concentration of ~40 μM. The standard deviations of these calcium distributions were higher toward the edges of the active zones, as would be expected, with values comparable to the mean at the center of the zone and much greater than the mean toward its edges (Fig. 2, *Ca* and *Da*). This was much the same for the calcium bound to the mobile and fixed buffers, except that the standard deviation was substantially less than the mean at the center of the zones (standard deviations for each of the cases in Fig. 2, *A* and *B* are shown in the corresponding panels in Fig. 2, *C* and *D*, respectively). Increasing the number of calcium ions that enters increases the number of calcium ions found in any region of the active zones as well as the number outside the zones, but the qualitative role of the mobile and fixed buffers remains the same as shown in Fig. 2: the endogenous buffers maintain a very small free calcium concentration in any region of the active zones.

Next, the effects of a low-affinity indicator such as furaptra and of a high-affinity indicator such as fura-2 on the spatial distribution of calcium ions in the square-shaped active zones after an action potential were considered. For both small (5 $\times$ 5) and large (9 $\times$ 9) active zones the effect of the fura-2 was to decrease the number of free calcium ions to much the same extent across the entire active zone, so that the small number normally observed at the edges is substantially reduced (compare Figs. 3 *Aa* and 2 *Aa*; also Figs. 3 *Ba* and 2 *Ba*) as well as that of the fixed buffer, which now principally only catches the calcium at the middle of the active zone (compare Figs. 3 *Ac* and 2 *Ac*; also Figs. 3 *Bc* and 2 *Bc*), with much now being taken out of this region by the indicator (compare Fig. 3 *Ad* and 2 *Ab*; also Fig. 3 *Bd* and 2 *Bb*). This was the case, as the principal effect of the indicator is to act as an additional mobile buffer, decreasing the effect of the endogenous mobile buffer (compare Figs. 3 *Ab* and 2 *Ab*; also compare Figs. 3 *Bb* and 2 *Bb*). Although the effects of using a low-affinity indicator like furaptra were qualitatively the same as those

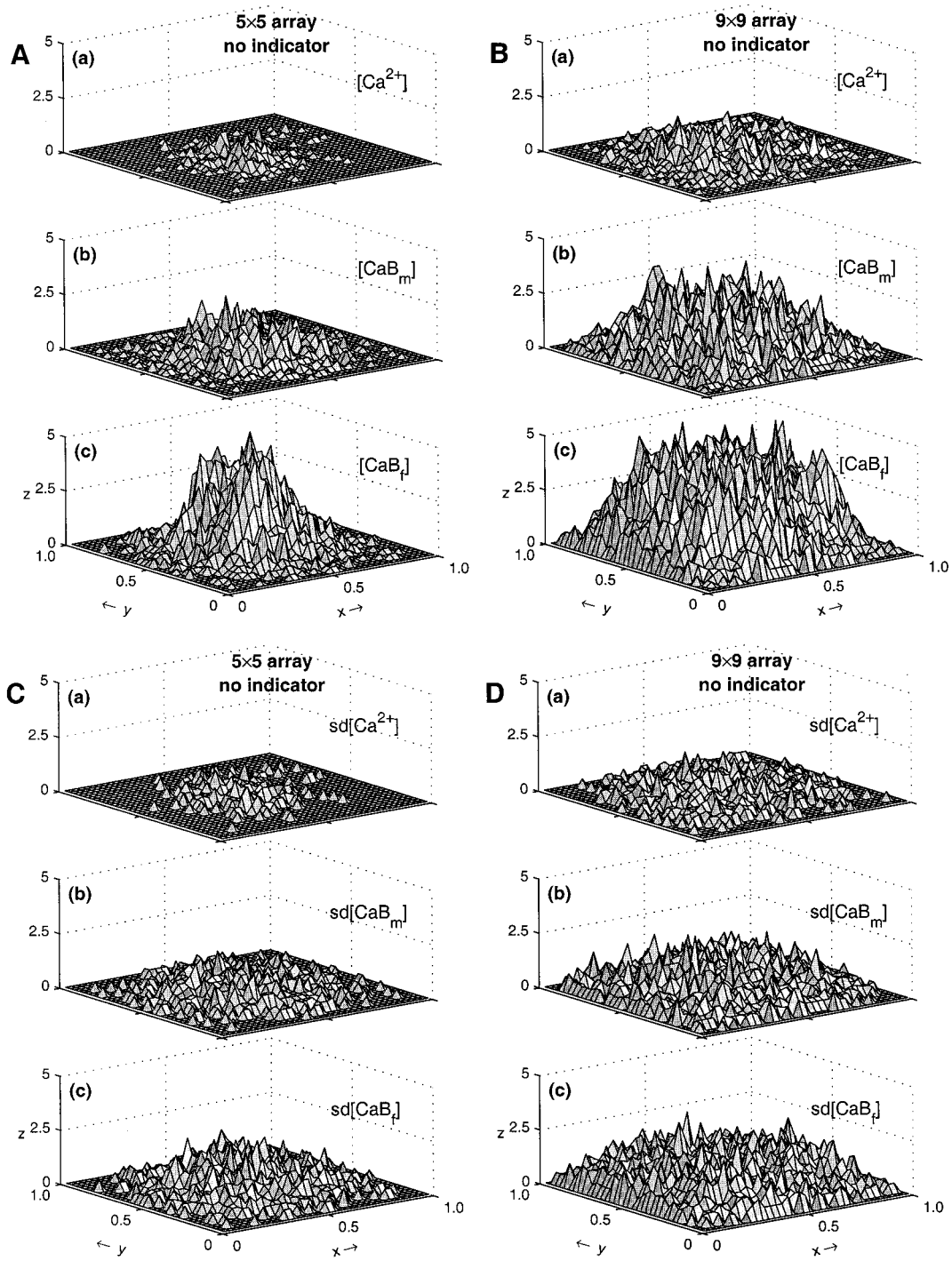

FIGURE 2 The spatial distribution of the mean and standard deviation of the calcium concentration at the presynaptic membrane of a varicosity or bouton following an action potential. The membrane has area 1 μm^2 and concentrations are calculated in the submembranous domain, taken to extend to a height of 30 nm above the membrane. The channels are spaced $100/\sqrt{2} \approx 70$ nm apart and arranged in a square grid in the middle of the presynaptic membrane, with 0.46 of these randomly activated during an action potential. The method for specifying the open time of the channels is described under Methods. The distributions are shown at the time when the average free calcium concentration is at its maximum. (In practice, this involved running the same simulation twice, once to get the peak and then to get the full spatial distribution. Typical times are 2.5 ms for the 5×5 array and 4.5 ms for the 9×9 array.) (*A*) Results for a 5×5 array of channels. (*B*) Results for a 9×9 array of channels. In each case, panels *a–c* give the concentrations of free calcium ($[Ca^{2+}]$), of calcium bound to the mobile buffer ($[CaB_m]$), and the calcium bound to the fixed buffer ($[CaB_f]$), respectively. These graphs show the mean of five calculations, each using the same pattern of channel openings, but with different random initializations of the Monte Carlo simulation. The coordinate system is such that the *x* and *y* axes are in the plane of the presynaptic membrane with the origin at one corner of the presynaptic membrane plane. The *z* coordinate gives the mean number of particles in the *xy* plane (to a depth of 30 nm), using a bin size of 30 nm square. The parameters used in the calculations are given in Table 1 of the accompanying article. (*C*, *D*) Standard deviations for the corresponding graphs in (*A*) and (*B*).

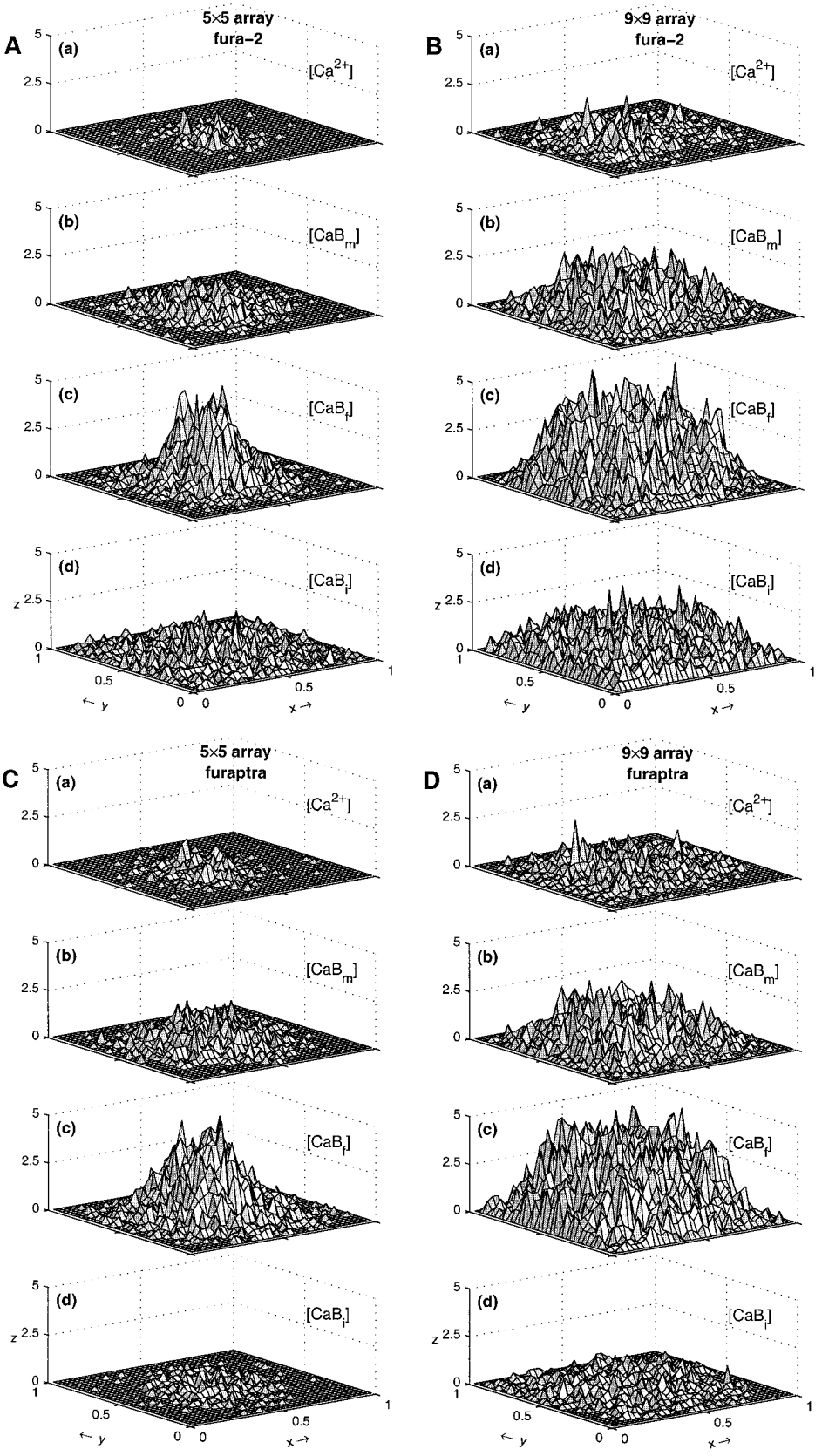

FIGURE 3 The spatial distribution of the mean of the calcium concentration at the presynaptic membrane of a varicosity or bouton in the presence of a calcium indicator following an action potential. The indicator used in (*A*) and (*B*) is fura-2, and that in (*C*) and (*D*) is furaptra. (*A*) and (*C*) give results for a 5 × 5 array of channels, (*B*) and (*D*) give results for a 9 × 9 array of channels. The details are as for Fig. 2, *A* and *B* with the addition that panel *d* in each case gives the concentration of calcium bound to the indicator ([CaB_i]).

for fura, they were quantitatively very different, as the former changed the effects of the endogenous buffers by <10%: see Fig. 3, *C* and *D* for the spatial distribution of calcium ions in the cases of a small (5 × 5) and a large (9 × 9) active zone, respectively, in the presence of the indicator furaptra.

In motor nerve terminals

Submembranous domains of calcium have also been considered for the case of active zones, such as those at motor nerve terminals, that possess calcium channels and vesicles on a line (Fig. 4; see also Fig. 8 *A*). A volume of cytosol made up of a square area of 1 μm × 1 μm of presynaptic membrane and taken to height of 30 nm from the membrane was again considered. In this case, calcium channels that occupied the active zone region were arranged along two parallel lines 30 nm apart, with the channels 50 nm apart on each line. The boundaries of the presynaptic membrane were again taken as enclosed by walls incorporating pumps, as given in the Methods section of Paper I. The frequency of N-channel opening under an action potential and the random spatial distribution of open channels were calculated as for Fig. 2. Fig. 4 shows the mean over five action potentials of the spatial distribution of the calcium ions at the time of peak calcium concentration in the volume under consideration. It will be noted that the mean number of calcium ions in any 30 nm is highest along the parallel line of channels (compare Fig. 4 *A* with Fig. 2 *Aa*). Although the average number of calcium ions is maintained at a low level by the fixed buffer (Fig. 4 *C*) and to a lesser extent by the mobile buffer (Fig. 4 *B*), these ions still amount to a high concentration, of the order of 50–100 μM, along the parallel lines of channels.

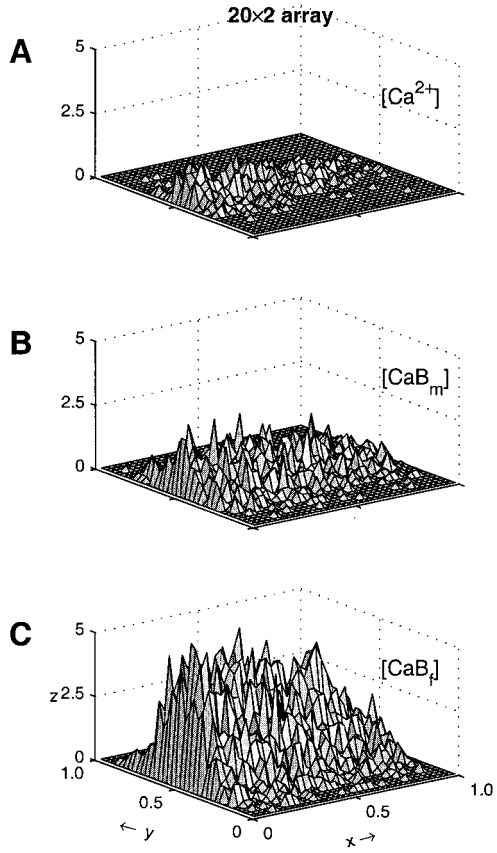

FIGURE 4 The spatial distribution of the mean of the calcium concentration at the active zone of an endplate's motor nerve terminal of area 1 μm^2 to a depth of 30 nm when calcium channels are arranged on two parallel lines in the middle of the presynaptic membrane, with the lines 30 nm apart and the channels 50 nm apart along the lines (cf. Fig. 8 *A* below) and 0.46 of these are activated in a spatially random array during an action potential. The density of the channels is thus 40 per 1000 nm. (*A*) The concentrations of free calcium ($[Ca^{2+}]$). (*B*) The concentration of calcium bound to the mobile buffer ($[CaB_m]$). (*C*) The concentration of calcium bound to the fixed buffer ($[CaB_f]$). The remaining details are as for Fig. 2 *A*.

During facilitation

The fixed buffer will gradually release its calcium after an impulse, allowing it to be transferred by diffusion or by the mobile buffer to the calcium pump at the plasma membrane. It was of interest to see what effect this would have on the calcium concentration at the presynaptic membrane due to a subsequent test impulse, especially given that the fixed buffer may be partially saturated by the calcium from the conditioning impulse, allowing more free calcium in the regions of the channels after a test impulse.

Fig. 5 shows the results for Monte Carlo calculations of the calcium after a test impulse (Fig. 5 *B*) 10 ms after a conditioning impulse (Fig. 5 *A*), in the presence of a low-affinity indicator, such as furaptra, that does not excessively disturb the calcium dynamics. The active zone under investigation is that of a bouton or varicosity, similar to that in Fig. 2. At 10 ms there is clearly more free calcium present in the active zone (compare Fig. 5 *Ba* with *Aa*) due to the residual free calcium contribution by the conditioning impulse, even though the extent of calcium bound by the mobile buffer (compare Fig. 5 *Bb* with *Ab*) and that by the fixed buffer (compare Fig. 5 *Bc* with *Ac*) is slightly elevated. This increase in free calcium ions after the test impulse is reflected in the calcium bound to the furaptra indicator (compare Fig. *Bd* with *Ad*). The relative contributions of the mobile and fixed buffers to residual calcium will be further commented on below in relation to the effects of these on facilitation.

The effects of a conditioning impulse on the free calcium to be found at the active zones of motor-nerve terminals, with their parallel rows of channels, after a subsequent test impulse 10 ms later, are given in Fig. 6. It is apparent that there is residual calcium in the active zone, even when channels are restricted to two parallel lines, at the time of the test impulse (compare Fig. 6 *Ba* with *Aa*). Both the

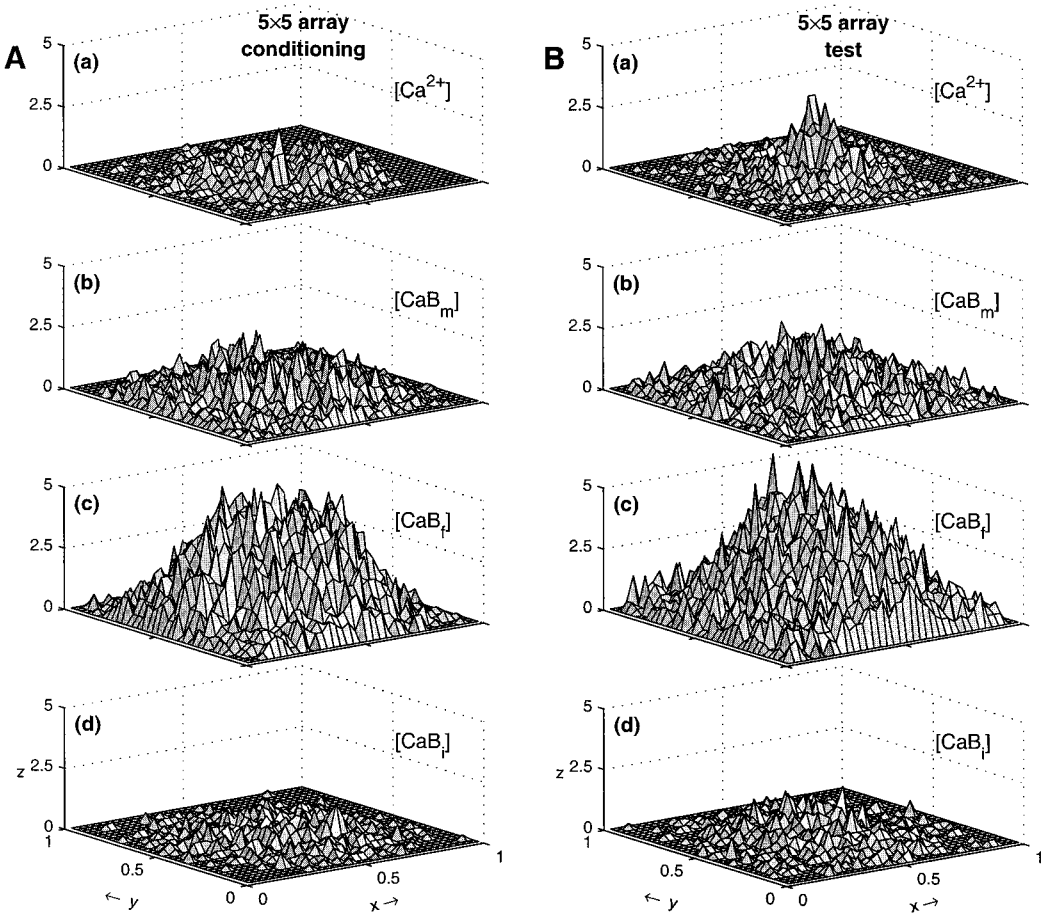

FIGURE 5 The spatial distribution of the mean of the calcium concentration at the presynaptic membrane of a varicosity or bouton in the presence of the calcium indicator furaptra after conditioning and test action potentials. The test action potential follows 10 ms after the conditioning action potential, and a different random choice of calcium channels was used in the test action potential from that used in the conditioning action potential. (*A*) Results for the conditioning action potential. (*B*) Results for the test action potential. The remaining details are as for Fig. 3 *C*.

mobile buffer (compare Fig. 6 *Bb* with *Ab*) and fixed buffer (compare Fig. 6 *Bc* with *Ac*) restrict the free calcium within the active zone for the conditioning and test impulses.

Exocytosis due to Ca^{2+}-submembranous domains in varicosities, boutons, and endplates

As mentioned in the Introduction, the concept of submembranous domains arises when there is nonindependence of exocytosis from secretory units. In this case, there is a superposition of effects arising from the summed contributions of calcium from several open channels within secretory units. In this section, the stochastic analysis of exocytosis in such submembranous domains is considered for different spatial distributions of secretory units, calcium channels, and synaptic vesicles in the active zones.

Arrays of secretory units

Active zones of varicosities and boutons. In this case, secretory units have been arranged into square arrays of the same kind used for the analysis of the free calcium in the submembranous region of nerve terminals in the previous section. Thus the vesicles of secretory units occupy arrays of from 5×5 up to 9×9 in the center of a 1 μm $\times$ 1 μm presynaptic membrane, as for the calcium channels in Fig. 2 (see Fig. 7 *A*). Two different secretory unit geometries are then considered: one in which the calcium channel is located 25 nm from its synaptic vesicle in the secretory unit and the other in which it is located 50 nm away (see Fig. 7 *A*, *upper* and *lower dotted boxes*, respectively). The spatial distribution of free calcium ions in the submembranous domain was then determined for these arrays after an impulse in the same way as before. In this case further Monte Carlo calculations were carried out to ascertain the extent of exocytosis in each region due to the rise in calcium in the domain.

After calcium influx, only about one or two vesicles on average underwent exocytosis of the 64 in the case of an 8×8 array (Fig. 7 *Ca*), and two examples of this for two individual impulses are shown in Fig. 7 *B*. These examples

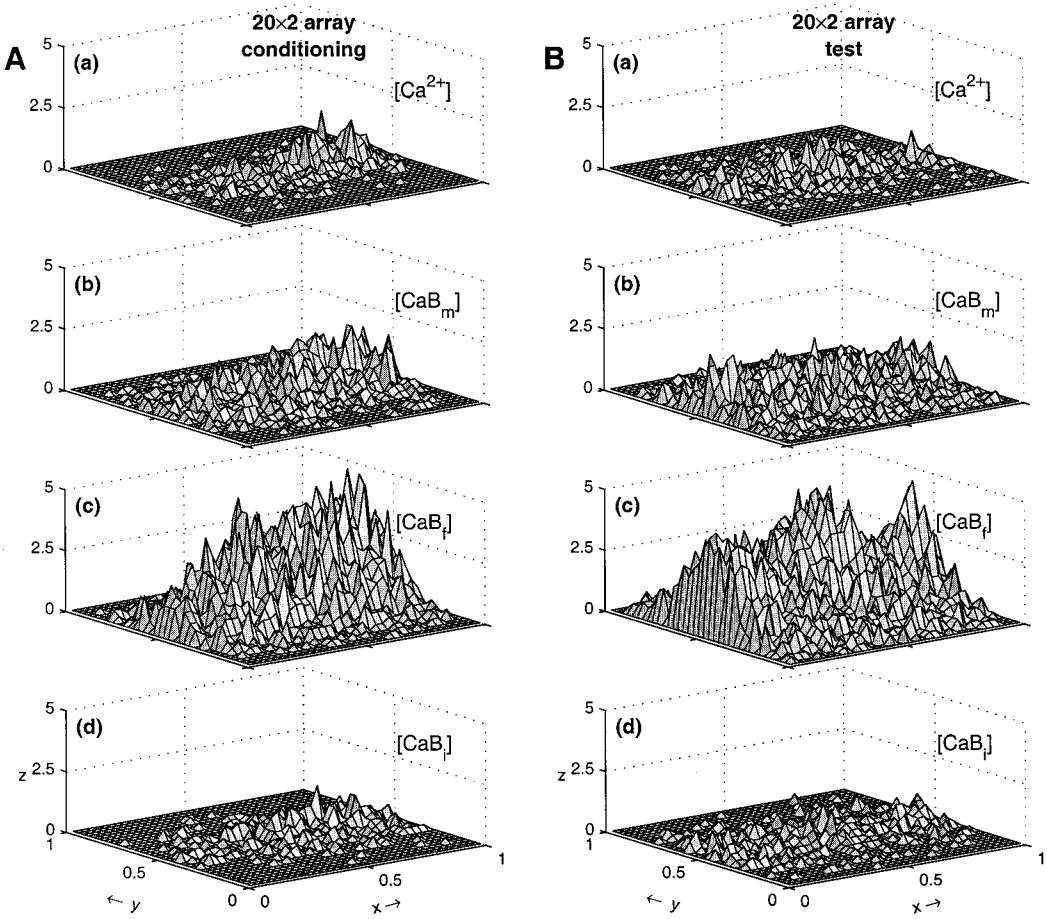

FIGURE 6 The spatial distribution of the mean of the calcium concentration at the active zone of an endplate's motor nerve terminal in the presence of a calcium indicator after conditioning and test action potentials. The array is as for Fig. 4 and the remaining details are as for Fig. 5.

indicate that while many calcium-sensor proteins in the array bound one or two calcium ions, only one or two bound four and triggered exocytosis. Exocytosis occurs throughout the array of vesicles (Fig. 7, *Ba* and *Bb*), reflecting the high free calcium in the region of the array (see Fig. 2). It was found that the spatial distribution of exocytosis within the active zone and the extent of exocytosis were little affected by the position of the channels in the secretory units. The extent of exocytosis for the case in which channels were 50 nm away from a synaptic vesicle in an array (Fig. 7 *Ca*, *closed squares*) was much the same as that for the usual case in which this distance was 25 nm (Fig. 7 *Ca*, *open squares*).

The question of how the extent of exocytosis changes with the size of the array that constitutes the active zone was also addressed. Fig. 7 *Ca* shows that as the active zone increases from an array of 5×5 secretory units to one of 9×9 secretory units, the average quantal release increases from near zero to ~3.5. This increase is steeper than linear, indicating a nonlinear relation between quantal release and the size of the active zone, which is to be expected if the secretory units use pooled and local calcium. (This is further analyzed below.) Quantal release is thus primarily determined for active zones consisting of a rectangular array of secretory units by the submembranous calcium concentration. It should be noted, however, that when the distance between the channel and the vesicle in the secretory unit is increased from the standard value of 25 nm to 50 nm, the average quantal release from an active zone of a given size is slightly smaller (Fig. 7 *Ca*, where the open squares are for 25 nm and the filled squares are for 50 nm). Such a result is to be expected if the pooled calcium from all the open channels in the active zone makes by far the major contribution to the calcium concentration at a vesicle's calcium-sensor, but that of a nearby open channel may be considered to make a special contribution.

Doubling the calcium influx allowed through channels produces an extremely high level of exocytosis, in which on average ~12 vesicles undergo exocytosis in the 8×8 case (Fig. 7 *Cb*). Virtually all calcium sensors in the 8×8 array bind a calcium ion, with many binding two and three, and ~12 binding four and going through to exocytosis. Again,

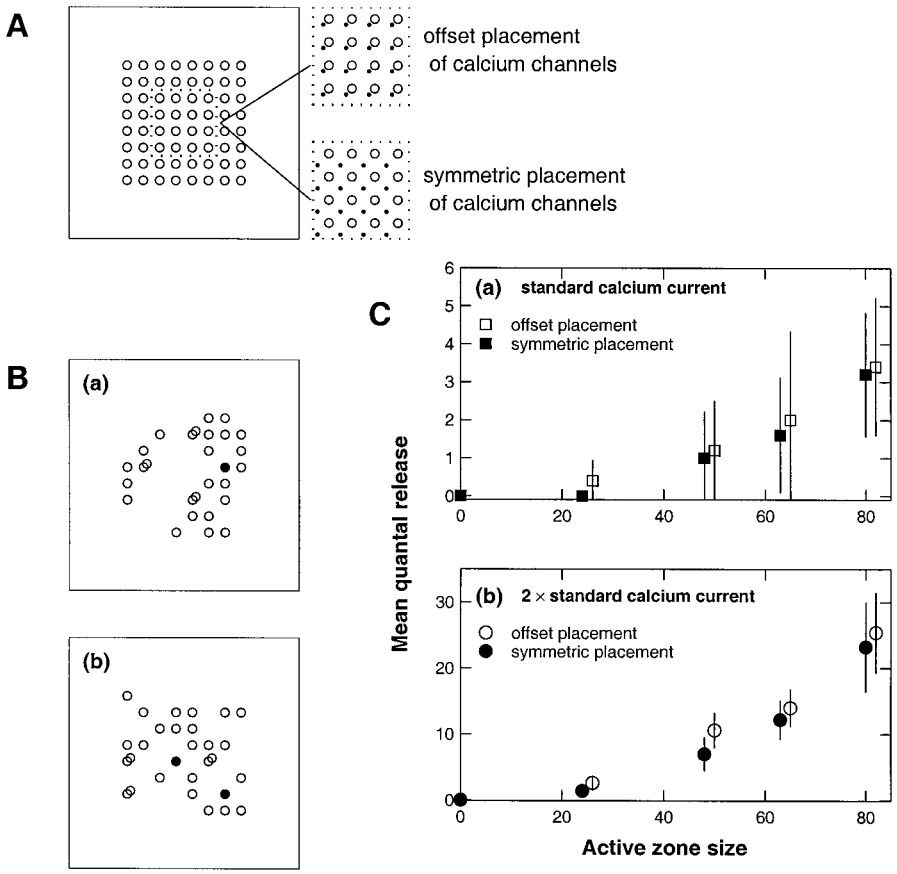

FIGURE 7 The frequency of secretion of quanta from a set of secretory units in a varicosity or bouton on the arrival of an action potential. (*A*) A set of 64 secretory units arranged at the presynaptic membrane in a square array, with the secretory units separated by 70 nm along the *x* and *y* axes. The vesicles are shown as open circles, and the dotted boxes also show the channels for the two cases of offset placement (channel-vesicle distance of 25 nm) and symmetric placement (channel-vesicle distance of 50 nm). (*B*) Two examples of the spatial distribution of vesicles that have undergone exocytosis (*filled circles*) or that have bound one (*single circle*) or two (*overlapping circles*) calcium ions. (Up to four calcium ions can be bound, but there are no three- or four-binding cases in these examples.) Results are shown at a time of 5.5 ms after the initiation of the action potential. (*C*) The relation between the size of the active zone (given as the total number of secretory units) and the extent of quantal secretion (given as the average number of exocytotic events or mean quantal release) from the array after an action potential. Panel *a* gives the quantal secretion for standard calcium current and for when the secretory units possess calcium channels at 25 nm from the vesicle [*open square*; see "offset placement" in (*A*)] or at 50 nm from the vesicle [*filled square*; see "symmetric placement" in (*A*)]. Panel *b* gives the corresponding results for twice the standard calcium current. In each case, the results are the mean of five Monte Carlo simulations, each using a different random selection of channel openings as given under Methods. Standard deviations are shown. The parameters used in the calculations are given in Table 1 of the accompanying article.

there is a nonlinear relation between the size of the active zone, or number of secretory units in an array, and the extent of quantal secretion (Fig. 7 *Cb*). This emphasizes that there is a nonlocal interaction between the secretory units in these active zones.

Active zones of motor nerve terminals. In the case of an active zone of a motor nerve terminal, the vesicles are arranged on two parallel lines, separated by 80 nm, with the vesicles spaced 50 nm apart along the lines; calcium channels are also spaced 50 nm apart on lines parallel to the vesicle lines and separated from them by 25 nm, as shown in Fig. 8 *A*. Thus, in this case secretory units are restricted to two parallel lines 80 nm apart with the calcium channels that belong to a secretory unit 25 nm from its vesicle-associated protein (Fig. 8 *A*).

This geometry of secretory units and calcium channels conforms to the most likely arrangement to be found in amphibian motor-nerve terminals (see Introduction), in which the lines of secretory units can extend across the entire width of the presynaptic membrane of up to 1 μm. An active zone of this length possesses 40 vesicle-associated proteins that bind one or more calcium ions (Fig. 8 *B*), but only on an average of 62% of occasions did an impulse trigger exocytosis of a vesicle, although there were double and even triple exocytotic events, giving rise to a mean quantal release of ~1.0 (Fig. 8 *Ca*).

For active zone lengths >~16 secretory units the relation between the average quantal release from an active zone and the length of the active zone was approximately linear; for shorter active zones the quantal release was near to zero

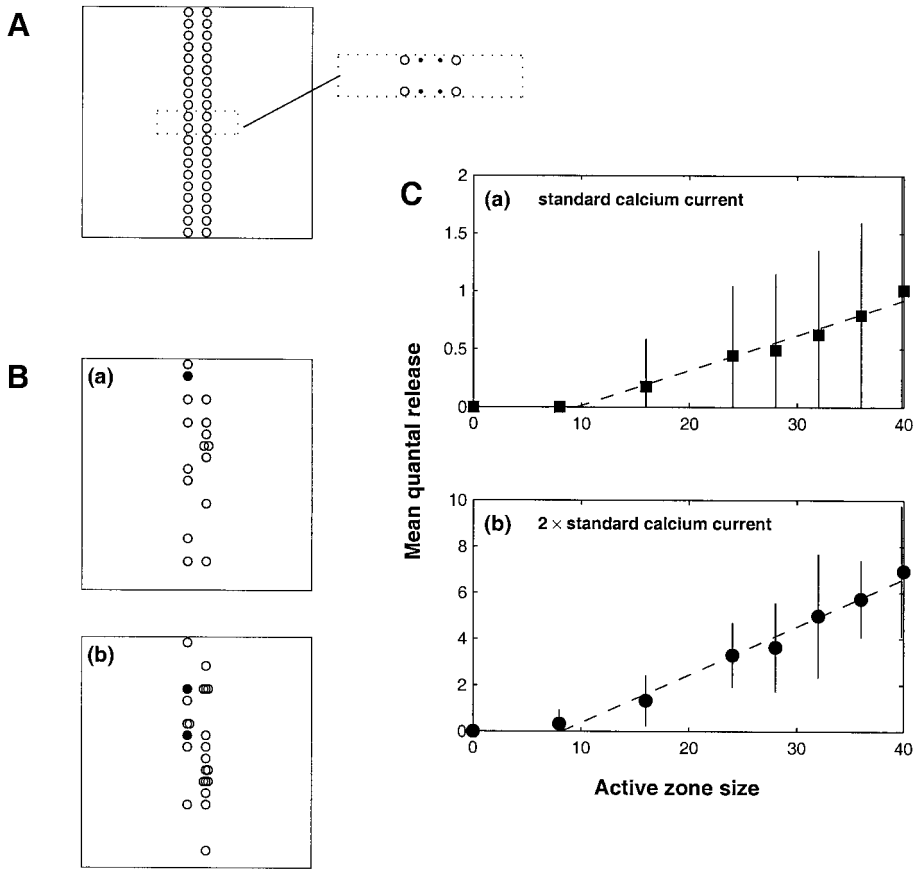

FIGURE 8 The frequency of secretion of quanta from a set of secretory units at the active zone of an endplate on the arrival of an action potential. (*A*) A set of secretory units arranged at the presynaptic membrane along two parallel lines in the middle of the presynaptic membrane of 1 μm $\times$ 1 μm, so that there are 40 secretory units present if the active zone extends across the entire width of the presynaptic membrane. The vesicles are shown as open circles in two lines 80 nm apart and the dotted box shows also the channels in two lines 30 nm apart, thus giving a channel-vesicle distance of 25 nm. (*B*) Two examples of the spatial distribution of vesicles that have undergone exocytosis (details as for Fig. 7 *B*). (*C*) The relation between the length of the active zone (given as the total number of secretory units, or active zone size) and the extent of quantal secretion (given as the average number of exocytotic events) from the array after an action potential. Panel *a* gives the quantal secretion for standard calcium current. Panel *b* gives the results for twice the standard calcium current. In each case, the results are the mean of up to 50 Monte Carlo simulations, using different random selections of channel openings. (More runs were required than for Fig. 7 because the different geometry increased the stochastic variability of the results.) The broken lines show linear fits to the points: see Eq. 2.

(Fig. 8 *Ca*). Thus the quantal release from an active zone was approximately proportional to the number of secretory units for length >16 secretory units, in contrast to the case of active zones, in which the secretory units are organized into rectangular arrays, in which case the increase in quantal release with the size of the active zone is steeper than linear (compare Figs. 8 *Ca* and 7 *Ca*). If the calcium current through the channels is increased by a factor of two, while keeping the same frequency distribution of channel open times under an action potential, then the much greater flux of calcium ions leads to almost an order of magnitude increase in the extent of exocytosis (compare Fig. 8 *Cb* with *Ca*). In this case, the near-linear relation between the quantal release and active zone length is evident for the endplate (Fig. 8 *Cb*) as is the nonlinear increase in quantal release with the size of the active zone in a bouton or varicosity (Fig. 7 *Cb*). It is interesting to note that the mean quantal release for active zones consisting of 40 secretory units on a double line is about the same as that for 40 secretory units in a rectangular array (compare Figs. 8 *C* and 7 *C*).

The secretory units in the motor-terminal active zones clearly do not act completely independently in the line case. If they did, the response (mean quantal release) for a line containing $2n$ secretory units would be $R_n = \alpha_0 n$, where α_0 is a constant (equal to the response from one pair of secretory units) and thus this line should pass through the origin, which it clearly does not in Fig. 8, *Ca* and *Cb*. Two effects can be present: one is the overlap between the calcium domains of neighboring pairs of secretory units; the other is the necessity for a certain level of calcium before appreciable exocytosis can occur. This suggests an expression of the form

$$R_n = 2\alpha_1 + (n - 2)\alpha_2 - \theta, \qquad (2)$$

where α_1 is the response from a secretory unit pair with one neighboring pair, α_2 is the response from a secretory unit pair with two neighboring pairs, and θ is a "threshold" term. (Eq. 2 holds if the right-hand side is greater than zero, otherwise R_n is zero.) R_n as given by Eq. 2 involves three parameters, α_1, α_2 and θ, and these cannot be uniquely determined by a linear fit to the data in Fig. 8 *C*. For the purposes of demonstrating that a choice of parameters is possible, assume that $\alpha_k = \alpha_0 + k\epsilon\alpha_0$, $k = 1, 2$, where ϵ is some number in the range $0 < \epsilon < 1$. Making the specific choice $\epsilon = 0.25$ gives the linear fits shown by the broken lines in Fig. 8 *Ca* ($\alpha_0 = 0.0403$, $\theta = 0.2692$) and Fig. 8 *Cb* ($\alpha_0 = 0.2763$, $\theta = 1.5574$).

In the planar case, similar reasoning (allowing for calcium overlaps between neighbors and for a threshold term) leads to the response from an $n \times n$ array being

$$R_{n\times n} = 4\alpha_3 + 4(n-2)\alpha_5 + (n-2)^2\alpha_8 - \theta, \qquad (3)$$

where α_k is the response from a secretory unit with k neighbors. (Again, this equation only holds for n sufficiently large so that the right-hand side is non-negative.) Thus, for a large enough array the response is of the form

$$R_{n\times n} = \beta_1 A + \beta_2\sqrt{A} + \beta_3, \qquad (4)$$

where $A = n^2$ is a measure of the area of the receptor patch and β_i are constants. For any reasonable values of the parameters, the $\sqrt{A}$ term does not cause much departure from linearity: certainly nowhere near as much as shown in Figs. 7 *C* and 9 *C*. For example, assuming $\alpha_k = \alpha_0 + k\epsilon\alpha_0$, taking $\epsilon = 0.25$ and fitting to the symmetric placement data

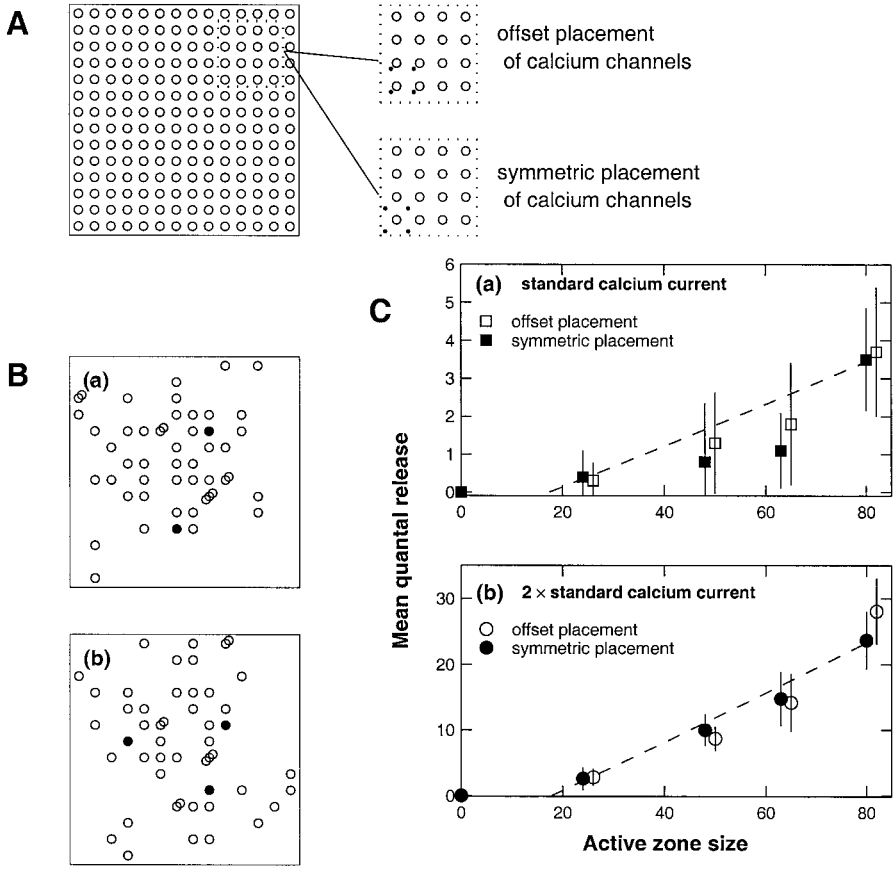

FIGURE 9 The frequency of secretion of quanta from a set of secretory units in a varicosity or bouton on the arrival of an action potential when there is an excess of vesicles over secretory units. (*A*) A set of 64 secretory units arranged at the presynaptic membrane in a square array, with the secretory units separated by 70 nm along the *x* and *y* axes, together with an extra three rows of vesicles around the perimeter; these extra vesicles possess calcium-sensor proteins and the capacity for exocytosis, but do not have associated calcium channels. The vesicles are shown as open circles, and the dotted boxes also show the channels for the two cases of offset placement (channel-vesicle distance of 25 nm) and symmetric placement (channel-vesicle distance of 50 nm). (*B*) Two examples of the spatial distribution of vesicles that have undergone exocytosis (details as for Fig. 7 *B*). (*C*) The relation between the size of the active zone (given as the total number of secretory units) and the extent of quantal secretion (given as the average number of exocytotic events) from the array after an action potential. Panel *a* gives the quantal secretion for standard calcium current and for when the secretory units possess calcium channels at 25 nm from the vesicle [*open square*; see "offset placement" in (*A*)] or at 50 nm from the vesicle [*filled square*; see "symmetric placement" in (*A*)]. Panel *b* gives the corresponding results for twice the standard calcium current. The broken lines show an attempt to fit the points using Eq. 3.

points at $n^2 = 25$ and $n^2 = 81$, gives the broken lines shown in Fig. 9, *Ca* and *Cb*. Over this range (Eq. 3) shows almost no departure from linearity, indicating that the nonlinearity in these figures does not arise from local overlap considerations. Instead, it appears to arise as a consequence of the pooled calcium from a large number of secretory units throughout the active zone contributing to the effects at each individual secretory unit.

Excess vesicles over secretory units

Active zones of varicosities and boutons. The possible effects of an excess of vesicles, with their associated proteins for exocytosis but without calcium channels, over secretory units in the active zone has also been investigated. Calculations have been performed for the situation in which vesicles are packed around a secretory unit array in an active zone with the same density as secretory units within the array, and this occurs over the entire presynaptic membrane of 1 μm $\times$ 1 μm (Fig. 9 *A*). In this case, there was no secretion outside the secretory unit array even though many calcium sensors associated with the vesicles outside of the array bound one or two calcium ions (Fig. 9 *B*). Undoubtedly this restriction of exocytosis to within the array was due to the action of the endogenous buffers restraining the high levels of submembranous calcium to within the active zone (Fig. 2). The spatial distribution of exocytosis over the presynaptic membrane in this case was then the same as that in the absence of an excess of vesicles. The quantal release then increased with an increase in the size of the active zone array of secretory units in the same way for the case of excess vesicles as in the absence of such an excess (compare Fig. 9 *Ca* with Fig. 7 *Ca*). This was so even when the calcium current through the channels was increased by a factor of two (compare Fig. 9 *Cb* with Fig. 7 *Cb*).

Some mention should be made here of the possibility that the form of the nonlinearity of the relationship between quantal release and the size of the secretory unit array depends on the extent to which the submembranous calcium is removed from the edges of the array by the endogenous buffers (see Fig. 2). It is possible that as the array size changes the extent of removal of calcium at the edges of the array is such as to give a proportionally smaller removal of calcium ions, and hence a larger number of vesicles in the array are exposed at the edges to calcium, giving a larger quantal release. To some extent a test of this proposition is provided by the case of excess vesicles: such an excess does not give rise to any additional exocytosis at the edges of the secretory unit array, with secretion still maintained within the secretory unit array as noted above (Fig. 9 *B*), presumably because vesicles at the edge of the array, at the time of peak submembranous calcium, interact with relatively few calcium ions (Fig. 2). These results suggest that the nonlinear relationship between the extent of quantal release and active-zone size arises from the interaction between the pooled calcium from the open channels within the array and the individual vesicle-associated calcium sensor proteins.

Active zones of motor nerve terminals. The effect on exocytosis of excess sets of vesicles and their associated vesicle-associated proteins, devoid of calcium channels, in the active zones of motor nerve terminals has also been calculated. These excess vesicles were placed on lines parallel to those in the active zone, as shown in Fig. 10 *A*. The existence of these vesicles did not much affect the extent of exocytosis (Fig. 10 *B*; also compare Fig. 10 *Cc* with *Ca*) as expected, given that the secretory units tend to only interact

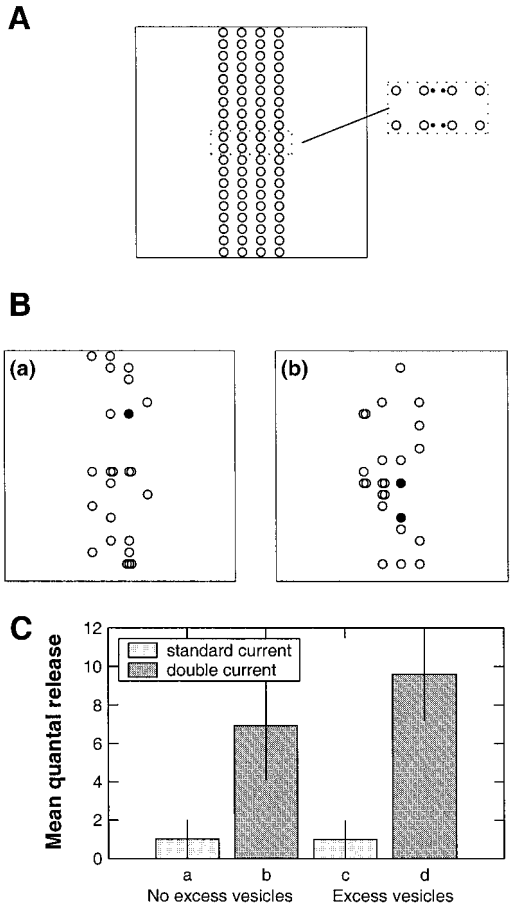

FIGURE 10 The frequency of secretion of quanta from a set of secretory units at the active zone of an endplate on the arrival of an action potential when there is an excess of vesicles over secretory units. (*A*) A set of secretory units arranged at the presynaptic membrane along two parallel lines in the middle of the presynaptic membrane of 1 μm $\times$ 1 μm, so that there are 40 secretory units present (cf. Fig. 8 *A*), together with an extra two rows of vesicles placed an equal distance on either side; these extra vesicles possess calcium-sensor proteins and the capacity for exocytosis, but do not have associated calcium channels. The vesicles are shown as open circles, and the dotted box also shows the channels. (*B*) Two examples of the spatial distribution of vesicles that have undergone exocytosis (details as for Fig. 7 *B*). (*C*) The mean number of exocytotic events after an action potential; *a* and *b* are for the case of no excess vesicles (as in Fig. 8 *A*) with standard calcium current and double calcium current, respectively; *c* and *d* are the corresponding results when excess vesicles are present.

locally in the active zone, and calcium from an open channel in a secretory unit is unlikely to have a significant impact at the calcium-sensor in one of the excess vesicles, given that the nearest such vesicle is 105 nm away. However, doubling the current through the channels did give a marginal increase in the extent of exocytosis (compare Fig. 10 *Cd* with *Cb*), so that in these circumstances some of the increased calcium influx does have an impact on the calcium sensors of the excess vesicles.

Excess channels over secretory units

Active zones of varicosities and boutons. The effect of the presynaptic membrane possessing an excess of N-type calcium channels outside of those belonging to secretory units in the array of the active zone has also been considered. Two extra rows of channels were placed in the presynaptic membrane outside of the active zone and with the same spacing as the secretory units within the active zone (Fig. 11 *A*). In this case, exocytosis occurred at the edges of the active zone and in the middle 50% of the zone (Fig. 11 *B*). This is to be expected, as the submembranous calcium now extends well beyond the edges of the zone (Fig. 2). Under these conditions, even the smallest array of secretory units considered, namely 5 × 5, gave relatively large average quantal releases under an impulse (~2) compared with this array size in the absence of an excess of channels (~0; compare Fig. 11 *D*, *e* and *g* with *a* and *c*). For the larger array of 8 × 8 this quantal release in the presence of an excess of channels reached ~7 (Fig. 11 *C*, *e* and *g*) compared with the control in the absence of such an excess of ~2 (Fig. 11 *C*, *a* and *c*). Such quantal releases are unrealistic when compared with experimental data (see Discussion) and suggest that it is unlikely that there is an excess of

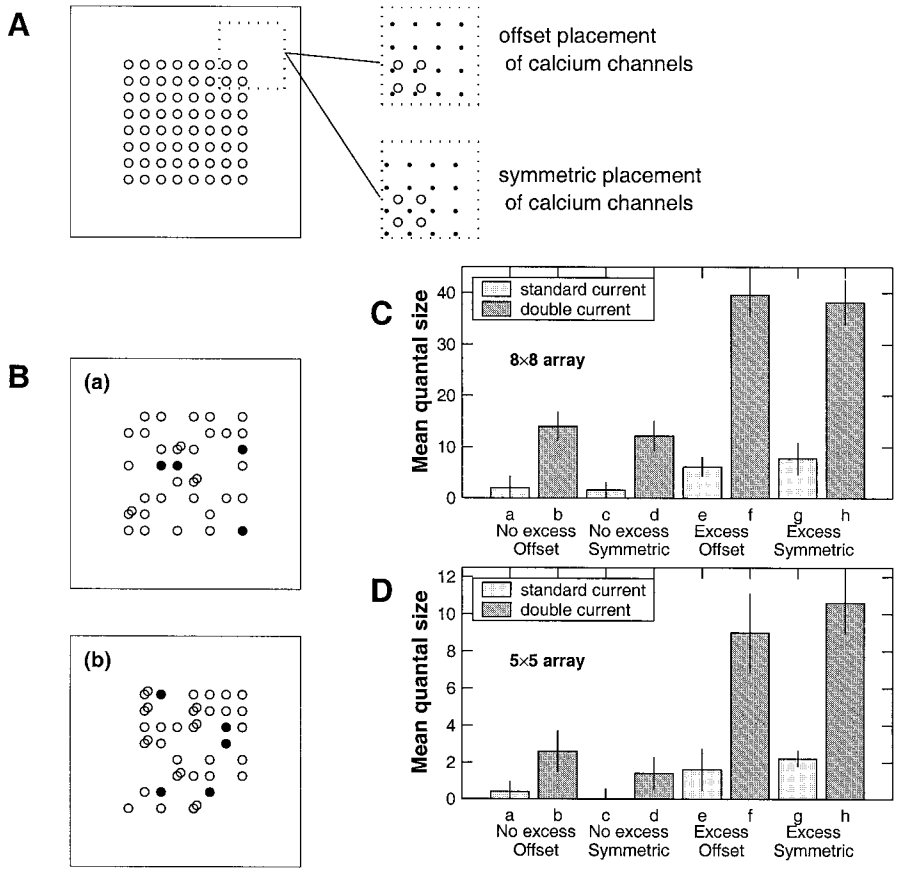

FIGURE 11 The frequency of secretion of quanta from a set of secretory units in a varicosity or bouton on the arrival of an action potential when there is an excess of N-type calcium channels over secretory units. (*A*) A set of 64 secretory units arranged at the presynaptic membrane in a square array, with the secretory units separated by 70 nm along the *x* and *y* axes. In addition, there are an extra two rows of calcium channels around the perimeter, placed either in the offset position (*upper dotted box*) or symmetrically (*lower dotted box*). (*B*) Two examples of the spatial distribution of vesicles that have undergone exocytosis (details as for Fig. 7 *B*). (*C*) The mean number of exocytotic events from an 8 × 8 array of secretory units after an action potential; *a* and *b* are for the case of no excess channels with offset placement of the calcium channels (Fig. 7 *A*, *upper dotted box*) with standard calcium current and double calcium current, respectively; *c* and *d* are the corresponding results for symmetric placing of the channels (Fig. 7 *A*, *lower dotted box*); *e* and *f* are the corresponding results for excess channels and offset placing of the channels (*A*, *upper dotted box*); *g* and *h* are the corresponding results for excess channels and symmetric placing of the channels (*A*, *lower dotted box*). (*D*) The same as for (*C*), except that the array of secretory units is reduced to 5 × 5.

calcium channels outside of the active zone. This becomes even more obvious when the calcium current is doubled through the channels, in which case quantal releases of between 10 and 40 are reached for active zone sizes of 5 × 5 and of 8 × 8, respectively (Fig. 11 *D*, *f* and *h*; Fig. 11 *C*, *f* and *h*).

Active zones of motor nerve terminals. The case was also considered of an excess of calcium channels outside the lines of secretory units that constitute the active zones of motor-nerve terminals. Excess channels were placed throughout the presynaptic membrane, either along lines parallel to those of the existing channels within the active zone (Fig. 12 *A*, *upper dotted box*) or interspersed between the existing channels (Fig. 12 *A*, *lower dotted box*). After an action potential there was an enormous increase in the quantal release over the case of the active zone without excess channels from a mean of 1.0 to a mean of ~8 (compare Fig. 12 *Cc* or *Ce* with *Ca*). This average quantal release in the presence of excess channels is so large compared with the experimentally determined quantal release that it suggests that such excess channels do not exist. This proposition is emphasized by consideration of the case when the calcium current through the channels is doubled (compare Fig. 12 *Cd* or *Cf* with Fig. 10 *Cb*).

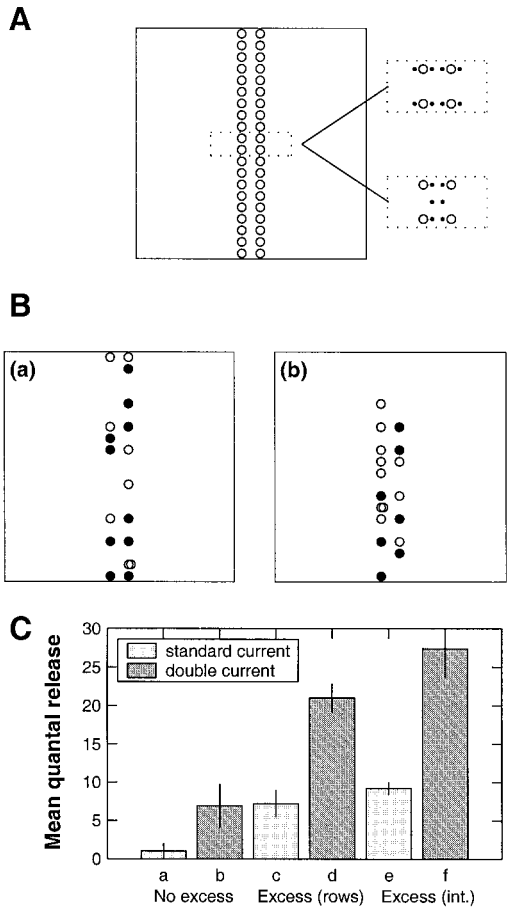

FIGURE 12 The frequency of secretion of quanta from a set of secretory units at the active zone of an endplate on the arrival of an action potential when there is an excess of N-type calcium channels over secretory units. (*A*) A set of 40 secretory units arranged along two parallel lines in the middle of the presynaptic membrane of size 1 μm × 1 μm (cf. Fig. 8 *A*), together with 40 extra calcium channels placed either as two rows at an equal distance on the other side of the vesicles (*upper dotted box*) or interspersed between the existing channels (*lower dotted box*). (*B*) Two examples of the spatial distribution of vesicles that have undergone exocytosis for the case of two extra rows of channels (details as for Fig. 7 *B*). (*C*) The mean number of exocytotic events after an action potential; *a* and *b* are for the case of no excess channels (as in Fig. 8 *A*) with standard calcium current and double calcium current, respectively; *c* and *d* are the corresponding results when excess channels are present as extra rows; *e* and *f* are the corresponding results when excess channels are interspersed between the original channels.

Test-conditioning sequences of impulses

Active zones of varicosities and boutons

It has been noted that after an action potential there is not only a residual free calcium concentration in the submembranous region that is removed from the cytosol by calcium pumps but also a transient occupation of the endogenous buffers by calcium ions in this region (Fig. 5). This last effect results in a large increase in the free calcium ions in the submembranous region if a subsequent test action potential occurs during this transient occupation of the endogenous buffers (Fig. 13 *A*), an increase well above that produced in the submembranous region by the conditioning action potential. The consequences of this for the release of quanta by the test action potential have been explored (Fig. 13 *B*). If the conditioning/test sequence occurs at an interval of 10 ms, then the average quantal release increases from 2.2 to 5.1 for a secretory unit array of 8 × 8, giving a facilitation of 1.32 (Fig. 13 *Ca*). If the calcium current through the channels is increased, as would occur with an increase in the external calcium concentration, then there is a decrease in the extent of facilitation, which in the case of the 8 × 8 array is from 1.32 in standard calcium to 1.06 in double calcium for offset calcium channels, and from 2.08 in standard calcium to 1.4 in double calcium for the centered channels. Such decreases in facilitation with an increase in external calcium concentration are observed experimentally.

Fig. 14, which is for the case of double calcium influx, shows that this facilitation is primarily due to the partial saturation of both the mobile (Fig. 14 *B*) and fixed (Fig. 14 *C*) buffers at the time of the test action potential, together with the saturation of the calcium pump at this time (Fig. 14 *D*) which continues to pump out calcium (Fig. 14 *E*). There is only a small contribution from the residual free calcium remaining from the conditioning pulse (Fig. 14 *A*) and virtually none from the buffering effects due to the vesicle-associated calcium sensors binding calcium ions (Fig. 14 *F*).

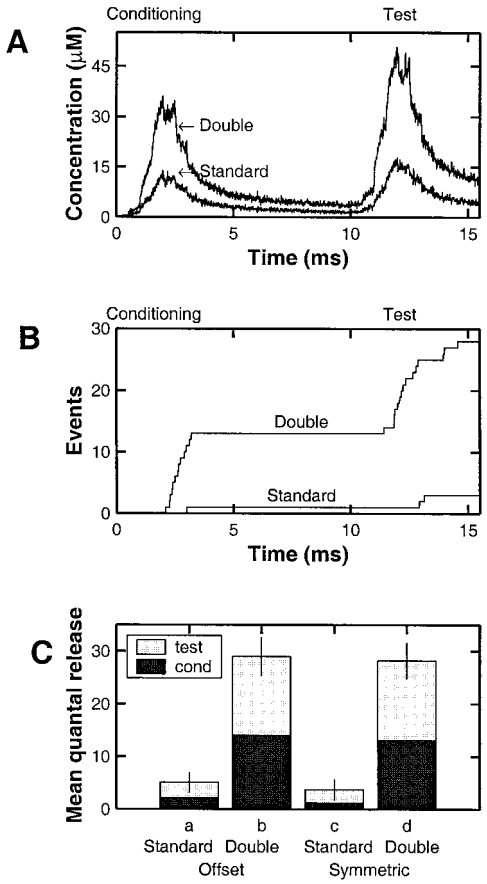

FIGURE 13 The frequency of secretion of quanta from a set of secretory units in a varicosity or bouton due to a test action potential arriving 10 ms after a conditioning action potential. The distribution of secretory units is the same as that given in Fig. 7 *A*. (*A*) The submembranous calcium concentration (given as the average concentration of free calcium ions in the 1 μm $\times$ 1 μm $\times$ 30 nm box) during the conditioning and the test impulse for both the case of standard calcium current (*lower curve*) and for twice that current (*upper curve*). (*B*) The extent and timing of exocytosis that accompanies these two different calcium currents for the conditioning and test action potentials. (*C*) The mean number of exocytotic events that occur as a result of the conditioning and test action potentials. Results shown are for 10 simulations: *a* and *b* are for the case of offset calcium channels (see Fig. 7 *A*, *upper dotted box*) for standard and double calcium current, respectively; *c* and *d* are the corresponding results for symmetric placement of the calcium channels (see Fig. 7 *A*, *lower dotted box*). In each case the dark shaded region shows the contribution from the conditioning impulse.

Active zones of motor-nerve terminals

Fig. 15 shows the corresponding results for active zones consisting of secretory units on a line. The behavior is similar to that shown for the 8 $\times$ 8 square array in Fig. 13, with a reduction in the mean quantal release, because now there are only 40 secretory units compared to 64 in Fig. 13. Fig. 15 *C* shows that there is facilitation from this process of 2.4 in low calcium and of 0.93 in high calcium. Fig. 16, which is for the case of double calcium influx, gives the details of binding to buffers and pumps (compare Fig. 14).

DISCUSSION

Calcium in the submembranous domain after the opening of multiple channels

Klingauf and Neher (1997) developed the concept of submembranous calcium in the context of their examination of how the relatively slow secretion of catecholamines occurs from chromaffin cells. One mechanism that might accomplish this involves most of the granules to be secreted not being located strategically close to a calcium channel, so that the pooled calcium from many open channels must reach the calcium sensor of the granules before exocytosis is triggered. This pooled calcium then constitutes the submembranous domain. In this case, rather than the microdomain of calcium dominated by fast diffusion dictating the temporal characteristics of the secretion process, the submembranous domain dominated by the slower buffering processes may determine the temporal characteristics of secretion. The submembranous domains of interest in the present work are those associated with varicosities and boutons, modeled on the assumption of rectangular arrays of channels in their active zones (Pfenninger et al., 1971), and those associated with amphibian motor-nerve terminals, possessing arrays of channels that are confined to two parallel lines in their active zones (Robitaille et al., 1990).

Deterministic solutions of the reaction-diffusion equations for rectangular arrays of channels show that there is a relatively high calcium concentration associated with the microdomains of each channel, superimposed on a lower calcium concentration due to the submembranous pooling of calcium from the different channels outside of the microdomains at the time of channel closure [see, for example Figs. 7 and 8 in Roberts (1994) and Fig. 3 in Klingauf and Neher (1997)]. However, when allowance is made for the stochastic opening of channels in the active zone under an action potential, the microdomains are not as distinct at the end of the action potential as in a deterministic solution, so that it is difficult to distinguish the microdomains from the submembranous calcium (see, for example, Fig. 3). This arises because many of the channels that open under the action potential do so for such a short time or at a time when the driving force on the calcium ions is so small that their microdomains are relatively small. However, as these are numerically the dominant kind of channel, they contribute significantly to the submembranous calcium, which then becomes comparable to the microdomains formed by the more effective channels.

There are very few submembranous calcium ions at the edge of the rectangular array of channels, with the mobile buffer carrying the ions out of the active zone region, as has been emphasized by Roberts (1994). However the "time averaged" simulation in his work giving rise to a "frozen" landscape of calcium concentration in the active zone consisting of microdomains associated with each open channel superimposed on a submembranous calcium according to a

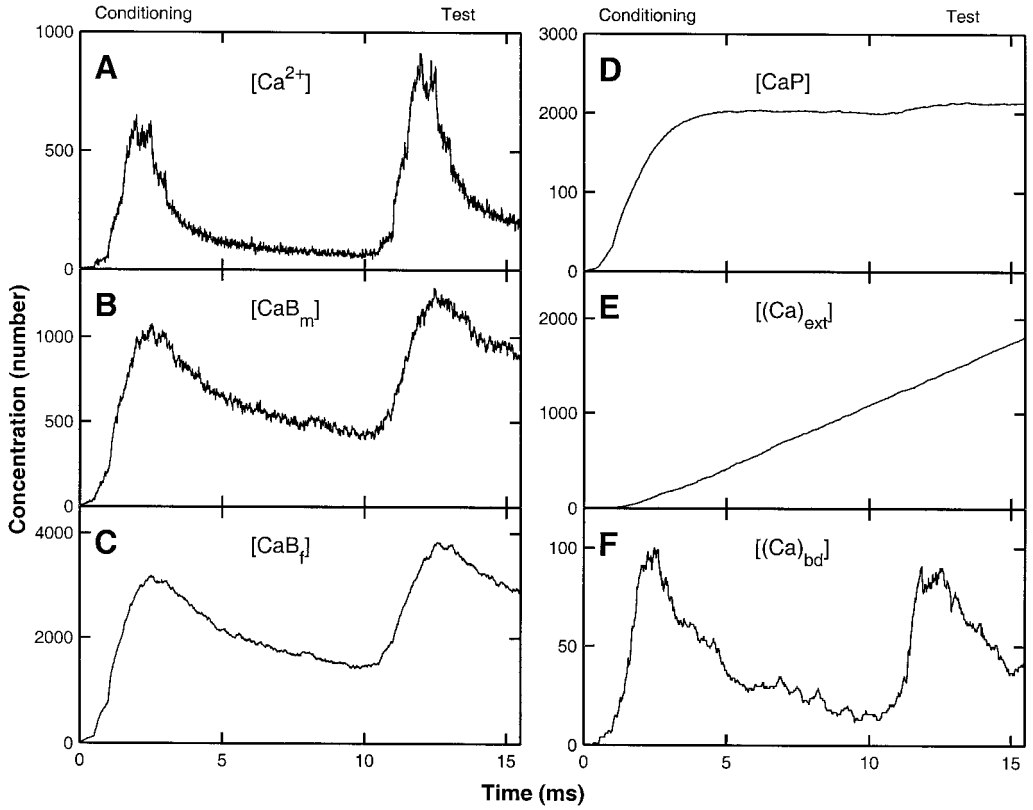

FIGURE 14 The distribution of calcium as a function of time due to a conditioning action potential followed by a test action potential 10 ms later. The details are as for Fig. 13 for the case of twice standard calcium current and offset placement of calcium channels. In each case the ordinate gives the concentration of either free or bound calcium ions in the submembranous region. (*A*) The number of free calcium ions. (*B*) The number of calcium ions bound to the mobile buffer. (*C*) The number of calcium ions bound to the fixed buffer. (*D*) The number of calcium ions bound to the pumps. (*E*) The number of calcium ions pumped out. (*F*) The number of calcium ions bound to the vesicle-associated proteins (not including those that have undergone exocytosis).

deterministic analysis, does not occur if a stochastic solution is obtained [compare Fig. 7 in Roberts (1994) with Fig. 2 *A* in this work]. The Monte Carlo analysis shows that the submembranous calcium is of the order of 50 μM in the middle of the rectangular arrays of channels, which is probably sufficient to activate the calcium sensors for exocytosis (Südhof, 1995). When the channels are arranged on a line, as in the active zone of motor-nerve terminals, the submembranous calcium is still significant compared with that of the microdomain calcium.

The temporal changes in increased efficacy of quantal release that occur at a nerve terminal when a test impulse follows a conditioning impulse at intervals of $<\sim$50 ms is referred to as F1 facilitation. The effect of a conditioning action potential on the spatiotemporal distribution of calcium in the submembranous domain after a subsequent test action potential within $\sim$10 ms is to elevate the free calcium ions in this domain. This arises principally as a consequence of the fixed and mobile buffers in the middle of the rectangular array of channels still retaining ions from the conditioning action potential, so that they are unavailable for binding ions entering during the test action potential (see also Klingauf and Neher, 1997). There is also some residual free calcium in the submembranous domain at this time from the conditioning action potential, but this adds only a small amount to that from the test action potential. The additional calcium after the test action potential due to part saturation of the buffers would contribute to the F1 phase of facilitation (Tanabe and Kijima, 1992).

Surprisingly, the additional free calcium ions available after a test action potential at motor-nerve terminals due to part-saturation of the buffers after the conditioning impulse are also significant. The microdomain calcium does not dominate the submembranous calcium at the active zones of endplates more than it does for the active zones of boutons and varicosities. The failure of the calcium chelator BAPTA to affect F1 facilitation at crayfish motor-nerve terminals (Winslow et al., 1994) or amphibian motor-nerve terminals (Robitaille and Charlton, 1991) is explained by the fact that it is the part-saturation of the endogenous buffers by the calcium influx due to the conditioning impulse rather than any residual free calcium from this impulse that is mainly responsible for F1 facilitation, together with the binding of calcium ions to calcium-sensor proteins that did not trigger

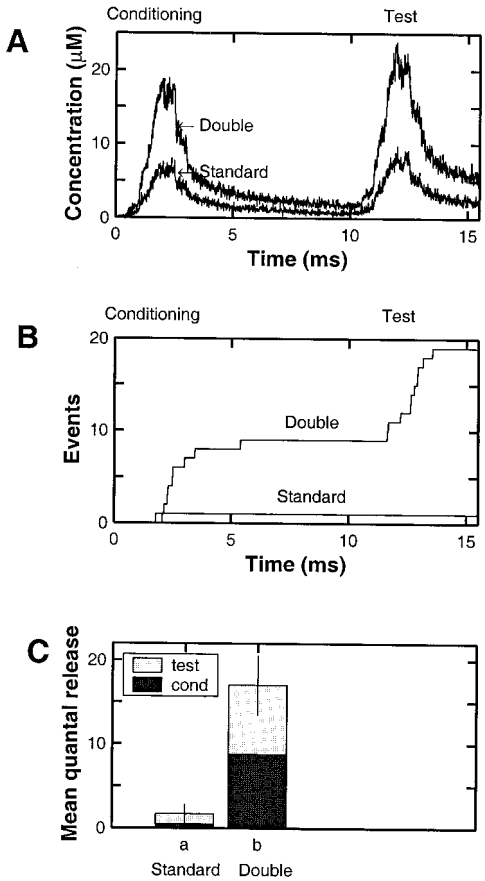

FIGURE 15 The frequency of secretion of quanta from a set of secretory units at the active zone of a motor nerve terminal due to a test action potential arriving 10 ms after a conditioning action potential. The distribution of secretory units is the same as that given in Fig. 8 *A*. The remaining details are as for Fig. 13.

exocytosis after the conditioning action potential (Bennett et al., 1997).

One question that arises is whether rectangular arrays of channels belonging to adjacent active zones can pool their calcium ions. Such an effect could lead to the nonindependence of adjacent active zones in the process of exocytosis (Bennett et al., 1998). Some deterministic calculations have been made that suggest that this might happen if the zones are within ~200 nm of each other and there is no mobile buffer (Cooper et al., 1996). The Monte Carlo simulations suggest that this is unlikely to occur in the presence of an endogenous mobile buffer, because the edges of the channel arrays are virtually devoid of any calcium ions as the buffer carries the ions away. The answer to the question of nonindependence then depends on whether there is a mobile buffer present.

The discovery that fast-acting buffers like BAPTA can modify transmitter release at motor-nerve terminals, whereas slower buffers such as EGTA cannot (Robitaille et al., 1993; Losavio and Muchnik, 1997) is explained by the fact that it is the high-concentration calcium microdomains dissipated primarily by diffusion that trigger transmitter release at these terminals, so that only BAPTA can modify them. However, if transmitter release is primarily through two-dimensional arrays of channels, then the submembranous calcium domains play a main role in triggering diffusion, and so EGTA can have an effect on these (Borst and Sakmann, 1996).

Quantal release at calcium submembranous domains

When there is a relatively large rectangular array of channels in the active zone, buffers ensure that calcium ions are found infrequently at the edges of the array after an action potential (Bennett et al., 1998). As a consequence, exocytosis is confined to the center of the array, and the addition of extra vesicles outside the array makes no difference to the extent of quantal release. In this case there is no independence of the secretory units, as foreshadowed in Paper I when considering the four secretory unit case, as with about half the channels opened the calcium-sensor within any one secretory unit can bind calcium ions from several of the surrounding open channels, these ions constituting the submembranous calcium. Thus, with an increase in the number of secretory units in the array there is a disproportionately larger increase in the number that undergo exocytosis. The probability of secretion at adjacent varicosities of sympathetic nerve terminals varies considerably (Lavidis and Bennett, 1993; Bennett, 1994). Measurements of the calcium transients in these adjacent varicosities after an impulse show that these also vary to a large extent, suggesting different size active zones with different numbers of secretory units in the adjacent varicosities (Brain and Bennett, 1997). However, there has been no comparison between the size of the active zones in the varicosities, identified, for example, by the relatively high concentrations of syntaxin found there (Brain et al., 1997), and the probability of secretion that would allow for a check of the proposal that this is highly nonlinear.

Multiquantal release at synapses

Whether the calcium microdomain is the sole source of calcium for triggering exocytosis, or whether contributions from the submembranous calcium must be considered, there is no limit in the present simulations on the possibility of multiquantal secretion from a synapse in the present models. The possibility that only one quantum might be capable of secretion from a synapse on the arrival of an action potential was first raised in the context of secretion at autonomic preganglionic nerve terminals for which the maximum number of quanta released from a single terminal during high calcium exposure was of the same order as the number of

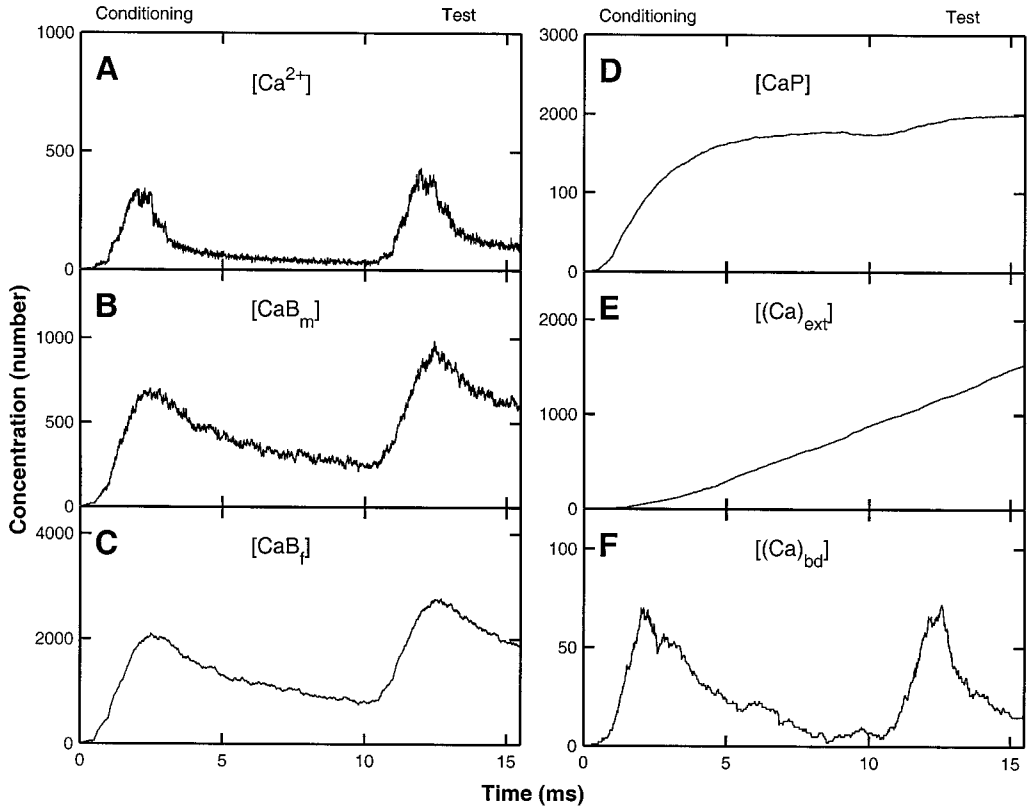

FIGURE 16 The distribution of calcium as a function of time at the active zone of a motor nerve terminal due to a conditioning action potential followed by a test action potential 10 ms later, for the case of twice standard calcium current (Fig. 15 *A*, *upper curve*). The remaining details are as for Fig. 14. (The scales on the ordinates have been kept the same as in Fig. 14 to facilitate comparison.)

synapses formed by the terminal; that is, the number of boutons that it formed on a single ganglion cell (Bennett et al., 1976). Recently this proposal has been especially promoted in relation to the release of quanta from boutons formed by hippocampal neurones in culture (Stevens and Wang, 1994; 1995; Murthy et al., 1997). Although there is considerable evidence for autoinhibitory mechanisms controlling quantal release due to the action of, for example, adenosine at motor-nerve terminals and preganglionic nerve terminals (Bennett et al., 1991; Bennett and Ho, 1991; van der Kloot, 1988), these do not autoinhibit quantal release within a single action potential, but rather during trains of action potentials. A study of whether there is an inhibitory mechanism for quantal release within an action potential, such that an early released quantum is followed by a refractory period during which later releases are inhibited, has not been found for quantal release at active zones of amphibian motor-nerve terminals (Thomson et al., 1995). Indeed, there is evidence for multiquantal spontaneous release measured with loose-patch electrodes over single varicosities of sympathetic nerve terminals (Bennett et al., 1996) and at single cerebellar boutons (Vincent and Marty, 1996). Given these caveats, a refractory mechanism for quantal release has not therefore been incorporated into the present simulations because there is an absence of direct experimental evidence for its existence.

This work was supported by an Australian Research Council Institutional Grant.

REFERENCES

Bennett, M. R. 1994. Quantal secretion from single visualized varicosities of sympathetic nerve terminals. *In* Molecular and Cellular Mechanisms of Neurotransmitter Release. L. Stjärne, P. Greengard, S. Grillner, T. Hökfelt, and D. Ottoson, editors. Raven Press, New York. 399–424.

Bennett, M. R., L. Farnell, and W. G. Gibson. 1998. On the origin of skewed distributions of spontaneous synaptic potentials in autonomic ganglia. *Proc. R. Soc. Lond. B.* 265:271–277.

Bennett, M. R., L. Farnell, and W. G. Gibson. 2000. The probability of quantal secretion near a single calcium channel of an active zone. *Biophys. J.* 78:2201–2221.

Bennett, M. R., T. Florin, and A. G. Pettigrew. 1976. The effect of calcium ions on the binomial statistical parameters that control acetylcholine release at preganglionic nerve terminals. *J. Physiol.* 257:597–620.

Bennett, M. R., W. G. Gibson, and J. Robinson. 1997. Probabilistic secretion of quanta and the synaptosecretosome hypothesis: evoked release at active zones of varicosities, boutons, and endplates. *Biophys. J.* 73:1815–1829.

Bennett, M. R., and S. Ho. 1991. Probabilistic secretion of quanta from nerve terminals in avian ciliary ganglia modulated by adenosine. *J. Physiol.* 440:513–527.

Bennett, M. R., S. Karunanithi, and N. A. Lavidis. 1991. Probabilistic secretion of quanta from nerve terminals in toad (*Bufo marinus*) muscle modulated by adenosine. *J. Physiol.* 433:421–434.

Bennett, M. R., J. Robinson, M. C. Phipps, S. Karunanithi, Y. Q. Lin, and L. Cottee. 1996. Quantal components of spontaneous excitatory junction potentials at visualized varicosities. *J. Aut. Nerv. Syst.* 56:161–174.

Borst, J. G. G., and B. Sakmann. 1996. Calcium influx and transmitter release in a fast CNS synapse. *Nature.* 383:431–434.

Brain, K. L., and M. R. Bennett. 1997. Calcium in sympathetic varicosities of mouse vas deferens during facilitation, augmentation and autoinhibition. *J. Physiol.* 502:521–536.

Brain, K. L., L. J. Cottee, and M. R. Bennett. 1997. Varicosities of single sympathetic nerve terminals possess syntaxin zones and different synaptotagmin N-terminus labeling following stimulation. *J. Neurocytol.* 26:491–500.

Cooper, R. L., J. L. Winslow, C. K. Govind, and H. L. Atwood. 1996. Synaptic structural complexity as a factor enhancing probability of calcium-mediated transmitter release. *J. Neurophysiol.* 75:2451–2466.

Delcour, A. H., D. Lipscombe, and R. W. Tsien. 1993. Multiple modes of N-type calcium channel activity distinguished by differences in gating kinetics. *J. Neurosci.* 13:181–194.

Heidelberger, R., C. Heinemann, E. Neher, and G. Matthews. 1994. Calcium dependence of the rate of exocytosis in a synaptic terminal. *Nature.* 371:513–515.

Heinemann, C., R. H. Chow, E. Neher, and R. S. Zucker. 1994. Kinetics of the secretory response in bovine chromaffin cells following flash photolysis of caged Ca^{2+}. *Biophys. J.* 67:2546–2557.

Heuser, J. E., and T. S. Reese. 1973. Evidence for recycling of synaptic vesicle membrane during transmitter release at the frog neuromuscular junction. *J. Cell Biol.* 57:315–344.

Klingauf, J., and E. Neher. 1997. Modeling buffered Ca^{2+} diffusion near the membrane: implications for secretion in neuroendocrine cells. *Biophys. J.* 72:674–690.

Lavidis, N. A., and M. R. Bennett. 1993. Probabilistic secretion of quanta from visualized varicosities along single sympathetic nerve terminals. *J. Aut. Nerv. Syst.* 43:41–50.

Losavio, A., and S. Muchnik. 1997. Spontaneous acetylcholine release in mammalian neuromuscular junctions. *Am. J. Physiol. Cardiovasc. Physiol.* 273:C1835–C1841.

Murthy, V. N., T. J. Sejnowski, and C. F. Stevens. 1997. Heterogeneous release properties of visualized individual hippocampal synapses. *Neuron.* 18:599–612.

Pfenninger, K., K. Akert, H. Moor, and C. Sandri. 1971. Freeze-fracturing of presynaptic membranes in the central nervous system. *Phil. Trans. R. Soc. Lond. B.* 261:387–388.

Pfenninger, K., K. Akert, H. Moor, and C. Sandri. 1972. The fine structure of freeze-fractured presynaptic membranes. *J. Neurocytol.* 1:129–149.

Roberts, W. M. 1994. Localization of calcium signals by a mobile calcium buffer in frog saccular hair cells. *J. Neurosci.* 14:3246–3262.

Robitaille, R., E. M. Adler, and M. P. Charlton. 1990. Strategic location of calcium channels at transmitter release sites of frog neuromuscular synapses. *Neuron.* 5:773–779.

Robitaille, R., and M. P. Charlton. 1991. Frequency facilitation is not caused by residual ionized calcium at the frog neuromuscular junction. *Ann. NY Acad. Sci.* 635:492–494.

Robitaille, R., M. L. Garcia, G. J. Kaczorowski, and M. P. Charlton. 1993. Functional colocalization of calcium and calcium-gated potassium channels in control of transmitter release. *Neuron.* 11:645–655.

Stevens, C. F., and Y. Wang. 1994. Changes in the reliability of synaptic function as a mechanism for plasticity. *Nature.* 371:704–707.

Stevens, C. F., and Y. Wang. 1995. Facilitation and depression at single central synapses. *Neuron.* 14:795–802.

Südhof, T. C. 1995. The synaptic vesicle cycle: a cascade of protein-protein interactions. *Nature.* 375:645–653.

Tanabe, N., and H. Kijima. 1992. Ca(2+)-dependent and -independent components of transmitter release at the frog neuromuscular junction. *J. Physiol.* 455:271–289.

Thomson, P. C., N. A. Lavidis, J. Robinson, and M. R. Bennett. 1995. Probabilistic secretion of quanta at somatic motor-nerve terminals: the fusion-pore model, quantal detection and autoinhibition. *Phil. Trans. R. Soc. Lond. B.* 349:197–214.

van der Kloot, W. 1988. Estimating the timing of quantal releases during end-plate currents at the frog neuromuscular junction. *J. Physiol.* 402: 595–603.

Vincent, P., and A. Marty. 1996. Fluctuations of inhibitory postsynaptic currents in Purkinje cells from rat cerebellar slices. *J. Physiol. (Lond.).* 494:183–199.

Westerbroek, R. E., T. Sakurai, E. M. Elliot, J. W. Hell, T. V. B. Starr, T. P. Snutch, and W. A. Catterall. 1995. Immunochemical identification and subcellular distribution of the α_{1A} subunits of brain calcium channels. *J. Neurosci.* 15:6403–6418.

Winslow, J. L., S. N. Duffy, and M. P. Charlton. 1994. Homosynaptic facilitation of transmitter release in crayfish is not affected by mobile calcium chelators: implications for the residual ionized calcium hypothesis from electrophysiological and computational analyses. *J. Neurophysiol.* 72:1769–1793.